

A unique photoemission method to measure semiconductor heterojunction band offsets

Q. Zhang, R. Li, R. Yan, T. Kosel, H. G. Xing et al.

Citation: *Appl. Phys. Lett.* **102**, 012101 (2013); doi: 10.1063/1.4772979

View online: <http://dx.doi.org/10.1063/1.4772979>

View Table of Contents: <http://apl.aip.org/resource/1/APPLAB/v102/i1>

Published by the [American Institute of Physics](#).

Related Articles

The electrostatics of Ta₂O₅ in Si-based metal oxide semiconductor devices

J. Appl. Phys. **113**, 074102 (2013)

Experimental evidence and modeling of two types of electron traps in Al₂O₃ for nonvolatile memory applications

J. Appl. Phys. **113**, 074501 (2013)

Defect states characterization of non-annealed and annealed ZrO₂/InAlN/GaN structures by capacitance measurements

Appl. Phys. Lett. **102**, 063502 (2013)

The effect of defects and their passivation on the density of states of the 4H-silicon-carbide/silicon-dioxide interface

J. Appl. Phys. **113**, 053703 (2013)

Interfacial study and energy-band alignment of annealed Al₂O₃ films prepared by atomic layer deposition on 4H-SiC

J. Appl. Phys. **113**, 044112 (2013)

Additional information on *Appl. Phys. Lett.*


Journal Homepage: <http://apl.aip.org/>

Journal Information: http://apl.aip.org/about/about_the_journal


Top downloads: http://apl.aip.org/features/most_downloaded

Information for Authors: <http://apl.aip.org/authors>

ADVERTISEMENT



Does your research require low temperatures? Contact Janis today.
Our engineers will assist you in choosing the best system for your application.



10 mK to 800 K
Cryocoolers
Dilution Refrigerator Systems
Micro-manipulated Probe Stations

LHe/LN₂ Cryostats
Magnet Systems

sales@janis.com www.janis.com
Click to view our product web page.

A unique photoemission method to measure semiconductor heterojunction band offsets

Q. Zhang,^{1,2} R. Li,² R. Yan,^{1,2} T. Kosel,² H. G. Xing,² A. C. Seabaugh,² K. Xu,^{1,3}
 O. A. Kirillov,¹ D. J. Gundlach,¹ C. A. Richter,¹ and N. V. Nguyen^{1,a)}

¹Semiconductor and Dimensional Metrology Division, National Institute of Standards and Technology,
 Gaithersburg, Maryland 20899, USA

²University of Notre Dame, Notre Dame, Indiana 46556, USA

³Purdue University, West Lafayette, Indiana 47907, USA

(Received 15 November 2012; accepted 6 December 2012; published online 2 January 2013)

We report a unique way to measure the energy band offset of a heterojunction by exploiting the light absorption profile in the heterojunction under visible-ultraviolet internal photoemission. This method was used to determine the band alignment of W/Al₂O₃/n⁺InAs/p⁺Al_{0.45}Ga_{0.55}Sb heterojunctions that are of interest for tunnel field-effect transistors. The barrier heights from the InAs and Al_{0.45}Ga_{0.55}Sb valence band maxima to the Al₂O₃ conduction band minimum are found to be 3.24 eV ± 0.05 eV and 2.79 eV ± 0.05 eV, respectively, yielding a 0.4 eV ± 0.1 eV offset at the InAs/AlGaSb interface. This approach can readily be applied to characterize a wide range of other semiconductor heterojunctions.

© 2013 American Institute of Physics. [<http://dx.doi.org/10.1063/1.4772979>]

The tunneling field-effect transistor (TFET) is one of the leading contenders to reduce power dissipation and extend performance of integrated circuits.^{1,2} In particular, III-V heterojunction TFETs have been designed,^{3–5} demonstrated,^{6–10} and projected^{11,12} to lower power dissipation relative to the scaled metal-oxide-semiconductor (MOS) FET. The tunnel current in the heterojunction TFETs is critically dependent on the barrier heights and band-offsets in these complex heterostructures. In this Letter, we report a unique way to measure this barrier height by controlling and exploiting the light absorption depth and the optical responses in the heterojunction under visible-ultraviolet internal photoemission (IPE).

IPE spectroscopy is a well-known, non-destructive technique to measure the energy barrier height at MOS interfaces.^{13–16} For semiconductor heterojunctions, it appears that IPE can be adapted in a straight forward fashion. In fact, with a free electron laser (FEL) as an excitation source, IPE has been reported using the tunability and intense peak power of the FEL in the infrared (IR) range to study band discontinuities of a host of heterojunctions including ZnSe/GaAs, ZnMgSSe/GaAs, GaAlAs/GaAs, CdS/CdTe, and InAs/AlSb.¹⁷ In the case of MOS structures, IPE model commonly used in interpreting experimental data follows Powell's model,²¹ which combines the optical excitation process in the emitter (semiconductor or metal) with Fowler's classical electron transmission model¹⁸ or escape probability of electrons injected from a solid surface to vacuum. However, this common model might not be proper when used to analyze the heterojunction IPE data because of the epitaxial nature of its interface as opposed to the amorphous/crystalline characteristics of the MOS interface. Another practical inconvenience in the analysis of III-V heterojunction TFETs is that because of the low band offsets, the typical IPE spectral range, from the near IR through the visible to the ultraviolet, is not sufficient, and a more elaborate

and sophisticated IR system operated at low temperature is required, such as FEL-IPE. To circumvent these complications, we will show that by measuring the band offset of each individual component of the junction with respect to a much larger band gap oxide, the low barrier height at the heterojunction can be ascertained. This approach was initially used to analyze a special case of a straddling semiconductor heterojunction in an earlier study where the structure layout serendipitously happened to follow this concept.¹⁹ In the following, we will delineate this unique technique and apply it to the determination of the band alignment of the W/Al₂O₃/n⁺InAs/p⁺AlGaSb TFET. In addition, another important device parameter is the interface charge, which can be extracted from the band alignment.

The device structure and the setup of the IPE measurement are shown schematically in Fig. 1(a). The semiconductor heterojunction was grown by molecular beam epitaxy (MBE, Intelligent Epitaxy, Richardson, TX²⁰) with the following layers, starting from a p⁺GaSb substrate: 30 nm p⁺GaSb with doping $5 \times 10^{18} \text{ cm}^{-3}$; 40 nm of graded p⁺AlGaSb (consisting of 10 nm p⁺Al_{0.15}Ga_{0.85}Sb; 10 nm p⁺Al_{0.30}Ga_{0.70}Sb, and 17 nm p⁺Al_{0.45}Ga_{0.55}Sb with doping $1.0 \times 10^{19} \text{ cm}^{-3}$; and 3 nm undoped Al_{0.45}Ga_{0.55}Sb) and 12 nm n⁺InAs with doping $1 \times 10^{17} \text{ cm}^{-3}$. An 8 nm Al₂O₃

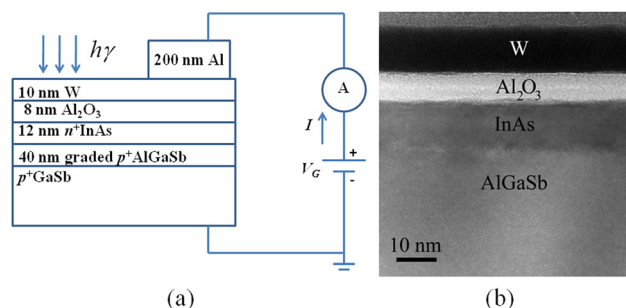


FIG. 1. (a) Schematic of the IPE measurement and (b) cross-sectional TEM image of a W/Al₂O₃/InAs/AlGaSb structure discussed by Li (see, Ref. 9).

^{a)}E-mail: nhan.nguyen@nist.gov.

gate dielectric was grown by atomic layer deposition (ALD) from trimethylaluminum and water at 300 °C, followed by a 10 nm tungsten (W) sputter deposition to create a semitransparent electrode for the IPE measurements. The cross-section of the sample structure was examined by transmission electron microscopy (TEM), Fig. 1(b), and the thicknesses of the Al₂O₃ and InAs layer were confirmed. The photocurrent was measured as a function of photon energy from 1.5 eV to 5.0 eV with the applied gate bias, V_G , varied from -1.0 to 1.2 V in steps of 0.1 V. The IPE yield was calculated as the ratio of the measured photocurrent to the incident light flux.

The oxide flat-band voltage, V_{FB} , is determined from V_G when the photocurrent switches direction from positive to negative.¹⁵ The flat-band voltage is found to be 0.2 V with respect to the grounded substrate. Shown in Fig. 2(a) is the cube root of IPE quantum yield versus photon energy at $V_G > V_{FB}$,^{13–16} where the electric field across the oxide is toward the semiconductor and estimated by $(V_G - V_{FB})/(\text{Al}_2\text{O}_3 \text{ thickness})$, assuming the gate voltage drop is inside the oxide. Following the classical Powell model,²¹ the cube root of IPE yield is assumed to be linear with photon energy above and near the spectral threshold (Φ). Since the barrier height at an oxide/AlSb (or GaSb) interface is lower than that of the same oxide/InAs interface,²² we can infer that the lower thresholds in Fig. 2(a) are the barrier heights from the Al_{0.45}Ga_{0.55}Sb valence band (VB) maxima to the Al₂O₃ conduction band (CB) minimum. When the photoemission yield contains features that can be identified with the inter-band critical points (CPs) of the dielectric function of the heterojunction materials, AlGaSb and InAs in this case, we can affirm the photoemission originates from that material.

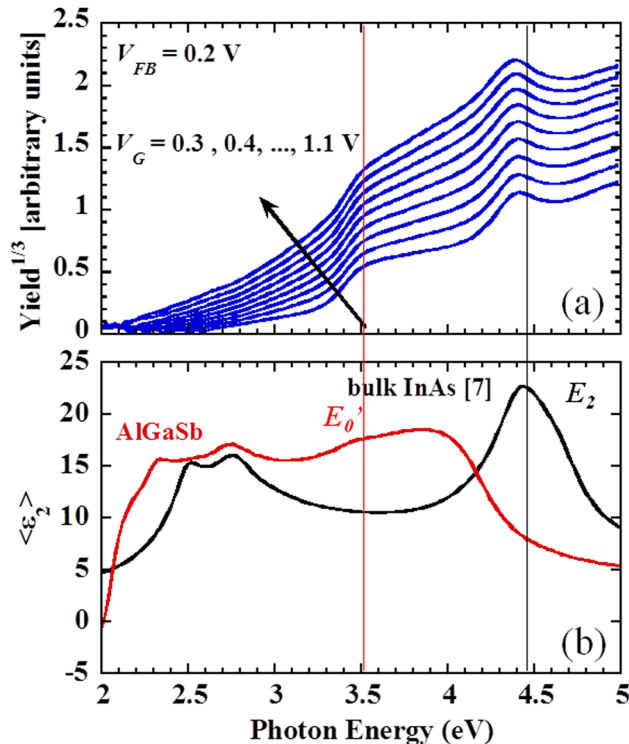


FIG. 2. (a) Cube root of the IPE yield as a function of photon energy for different gate bias. (b) Imaginary part (ϵ_2) of the pseudodielectric function of InAs (black) and AlGaSb (red), measured by spectroscopic ellipsometry.

Showing in Figure 2(b) are the dielectric functions of AlGaSb and InAs, measured by ellipsometry,^{13–15} indicating two particular CP's, E'_0 and E_2 , which are relevant to the IPE spectra depicted in Fig. 2(a). E'_0 and E_2 , respectively, correspond to the direct transitions from the valence band to the conduction band at Γ and X points in the Brillouin zone of momentum space.²³ In particular, the red line aligns with optical critical point E'_0 of AlGaSb to the decrease of the yield slope at ~ 3.5 eV, indicating the light penetrates beyond the 12 nm InAs layer into AlGaSb with photon energies at least up to 3.5 eV. The black line aligns the critical point E_2 to the field-independent dip at ~ 4.5 eV, implying the light is mainly absorbed by the InAs layer at higher photon energies as the penetration depth decreases. Therefore, the observed photoemission arises first from Al_{0.45}Ga_{0.55}Sb as the photon energy goes above the Al_{0.45}Ga_{0.55}Sb threshold, and then additional electrons are emitted from InAs as the photon energy increases above the InAs threshold. The increase of the yield^{1/3} slope at ~ 3.2 eV signifies the onset of the photoemission from the InAs layer over the Al₂O₃ barrier. We have thus shown that both barrier heights can readily be extracted, one from the InAs layer and the other from the AlGaSb substrate.

To further confirm the threshold energy assignments described above, we performed IPE on two additional devices, one with a much thicker (30 nm) InAs layer and the other with an ultrathin (less than 3 nm) InAs layer. Their corresponding cubic root yield plots are compared at the same oxide electric field with that of the 12 nm InAs device as displayed in Fig. 3. In the comparatively thick (30 nm) InAs layer (Fig. 3(a)), light penetration is limited to the InAs layer; thus only the optical feature of E_2 of InAs near 4.5 eV is observed. The photoemission comes from the InAs layer, and the threshold, Φ , near 3.2 eV is, therefore, the band offset between the InAs VB and the Al₂O₃ CB. On the other hand, in the sample with a much thinner InAs layer (less than 3 nm), only the bulk AlGaSb optical feature E'_0 near 3.5 eV is observed dominating in the photoemission spectrum (Fig. 3(b)). Therefore, the photoemission arises mainly from the AlGaSb layer, and thus the observed threshold, Φ , near 2.3 eV is indeed the band offset between the AlGaSb VB and the Al₂O₃ CB. Comparing these two thresholds with those extracted from the cube root yield plot in Fig. 3(c) for the 12 nm InAs device clearly confirms that: (i) the lower thresholds in Figs. 2(a) and 2(c) are, in fact, the barrier heights overcome by photoelectrons excited from AlGaSb, and (ii) the energies at which the yield^{1/3} slope begins to move upwards are the onset of emission by photo-excited electrons from InAs. The flat-band (zero-field) barrier heights Φ_0 of Al₂O₃ seen by AlGaSb and InAs are found to be 2.79 eV and 3.24 eV within 0.05 eV uncertainty, respectively. These zero-field values were extracted from the Schottky plot of barrier height vs. square-root oxide field (not shown) that expresses the linear dependence of barrier height on the square root of the oxide electric field.^{13–16}

A complete electron energy band diagram of the metal/oxide/semiconductor-heterojunction can be simulated by using the 1-D Poisson solver, BANDPROF.²⁴ In the simulation, we use the known band gaps and known relative dielectric constant of Al₂O₃ (6.8 eV, 0.8), InAs (0.35 eV, 14.6), and

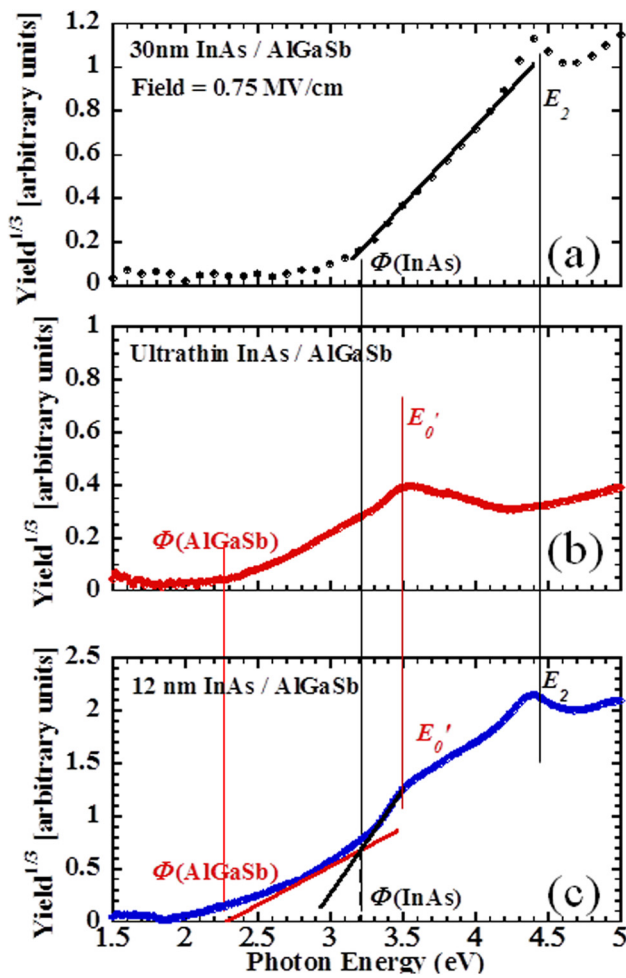


FIG. 3. Cube root of the IPE yield as a function of photon energy at electric field of 0.75 MV/cm for (a) 30 nm InAs layer, (b) ultrathin InAs layer, and (c) 12 nm InAs layer on AlGaSb/GaSb substrate.

$\text{Al}_x\text{Ga}_{1-x}\text{Sb}$ ($0.72 + 1.37x$ eV, $15.69 - 3.65x$), and the band offset values obtained from IPE measurements.

To satisfy the experimentally observed flat-band condition at $V_G = 0.2$ V, a negative charge at the interface between Al_2O_3 and InAs must be incorporated in the simulation, and the calculation results in an electron charge density of $1.2 \times 10^{12} \text{ cm}^{-2}$ accumulating the $\text{Al}_2\text{O}_3/\text{InAs}$ interface. Consequently, the detail of the band diagram at the flat-band condition can now be presented as shown in Fig. 4, where

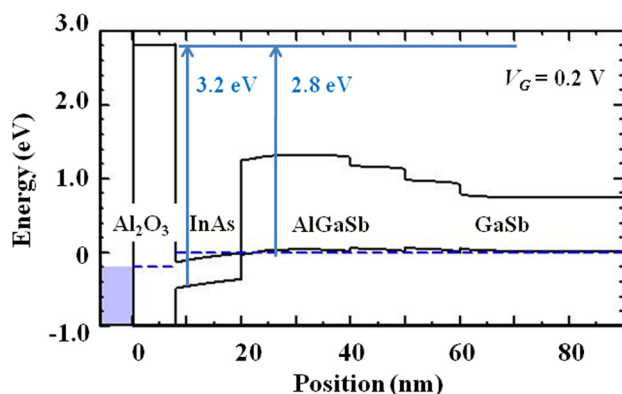


FIG. 4. Band diagram of the heterostructure at flat-band condition, simulated by BANDPROF (Ref. 24).

the band offsets determined from the IPE measurement are labeled accordingly, yielding a $0.4 \text{ eV} \pm 0.1 \text{ eV}$ offset at the $\text{InAs}/\text{Al}_{0.45}\text{Ga}_{0.55}\text{Sb}$ interface.

At this juncture, it is worthwhile to elaborate and discuss the unique IPE measurement method employed in this study that enables the determination of the band offsets at a semiconductor heterojunction. It is recognized that in order to measure the band offsets of heterojunctions in the visible photon energy range, the two necessary conditions should be arranged, so that the photoemission processes from the structure can be decoupled and reliably distinguished. First is the requirement of the thickness of the top semiconductor epitaxial layer lie in a certain range, which depends on its optical absorption or transmittance. The thickness must be thin enough to allow the light to penetrate into the deeper semiconductor layer, but thick enough to totally absorb the light at higher energies. The second criterion is the band offsets from semiconductor to the oxide are in the visible spectra range. The first requirement can be examined by calculating the transmittance (T) into the semiconductor substrate using a four-layer (metal/oxide/semiconductor epilayer/semiconductor substrate) model.²⁵ The complex optical refractive indexes of each material are experimentally measured by spectroscopic ellipsometry in this study.

By using the device structure in Fig. 1(a) as an example, we calculate the transmittance into the AlGaSb substrate as a function of photon energy as shown in Fig. 5 for different thicknesses of the InAs layer. It is apparent that the transmittance T into AlGaSb decreases with photon energy and with the increasing thickness of InAs: T is close to or above 10% for the full IPE spectra for the 3 nm InAs structures (red line); T is below 5% in the 30 nm InAs structures (black line) for photon energies above 2.7 eV. These two cases are extreme instances where photoemission is expected only from the AlGaSb substrate with a 3 nm InAs top layer and only from InAs with the 30 nm InAs top layer, consistent with what we observed in the IPE measurements, Figs. 3(a) and 3(b). For the case of the 12 nm InAs top layer, the transmittance into AlGaSb drops from more than 20% at low photon energies to below 10% as the photon energy increases above 4 eV (blue line). Since AlGaSb sees a lower barrier

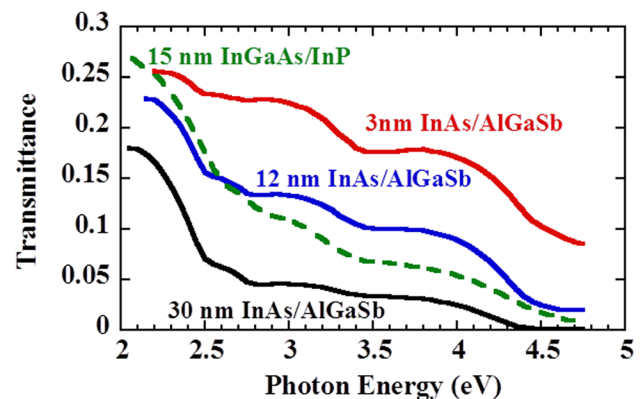


FIG. 5. The transmittance into the semiconductor substrate as a function of photon energy, calculated by a 4-layer model with metal (10 nm W), oxide (8 nm Al_2O_3), semiconductor epi-layer, and semiconductor substrate. The optical properties of each material are measured by spectroscopic ellipsometry.

than InAs, the photoemission is expected to arise first from AlGaSb at the low photon energy. At higher photon energy, the transmittance into AlGaSb drops and photon emission is expected to originate from InAs. Therefore, both barrier heights can be determined on the structure with this particular thickness of InAs. Incidentally, in retrospect, the structure W/Al₂O₃/InGaAs/InP in our previous work¹⁹ was also analyzed with the same rationality to arrive at two distinct thresholds from InGaAs and InP.²⁶

As a result of the analysis above, we believe that the approach can be extended to measure heterojunction band offsets of many other vertical TFET structures. In fact, in a vertical TFET design,^{5,8–10} the top semiconductor layer serves as the channel and to turn off the transistor its thickness is usually thin (~ 10 nm), and thus properly satisfies the stringent first requirement described above. To the extent of spectral photon energy accessibility, most TFETs are designed with high- k dielectrics with band gaps of 5–7 eV and band offsets to semiconductor VB of 2.5–3.5 eV that are suitable for IPE measurements. Therefore, it can be realized that most III-V TFET heterojunction band alignment can be experimentally resolved by IPE.

In conclusion, we have demonstrated that IPE measurement can be used to quantitatively characterize the multiple energy barriers of a heterojunction TFET. In particular, for this Al₂O₃/n⁺InAs/p⁺Al_{0.45}Ga_{0.55}Sb TFET structure, the cube root yield plot reveals the band offsets for both the top InAs layer and the underlying Al_{0.45}Ga_{0.55}Sb layer relative to the Al₂O₃. By combining the experimental data with the results of band diagram simulations, a self-consistent energy band diagram is derived at V_{FB} showing the necessary presence of an equivalent negative charge of $1.2 \times 10^{12} \text{ cm}^{-2}$ at the Al₂O₃/InAs interface. An approach proposes a specific design of a MOS heterojunction structure that enables IPE to uniquely measure the narrow band offsets at their interfaces, which would otherwise require a sophisticated low energy and low temperature photoemission setup.

The authors gratefully acknowledge the support of the NIST Semiconductor and Dimensional Metrology Division and the Nanoelectronics Research Initiative through the Midwest Institute for Nanoelectronics Discovery (MIND). The authors would also like to thank the NIST Center for

Nanoscale Science and Technology's Nanofab Facility for device fabrication support.

- ¹A. Seabaugh and Q. Zhang, *Proc. IEEE* **98**, 2095 (2010).
- ²A. M. Ionescu and H. Riel, *Nature* **479**, 329 (2011).
- ³M. Luisier and G. Klimeck, *Tech. Dig.—Int. Electron Devices Meet.* **2009**, 913.
- ⁴S. O. Koswatta, S. J. Koester, and W. Haensch, *IEEE Trans. Electron Device* **57**, 3222 (2010).
- ⁵Y. Lu, G. Zhou, R. Li, Q. Liu, Q. Zhang, T. Vasen, S. D. Chae, T. Kosel, M. Wistey, H. Xing *et al.*, *IEEE Electron Device Lett.* **33**, 655 (2012).
- ⁶D. Mohata, S. Mookerjee, A. Agrawal, Y. Li, T. Mayer, V. Narayanan, A. Liu, D. Loubichev, J. Fastenau, and S. Datta, *Appl. Phys. Express* **4**, 024105 (2011).
- ⁷G. Dewey, B. Chu-Kung, J. Boardman, J. Fastenau, J. Kavalieros, and R. Kotlyar, *Tech. Dig.—Int. Electron Devices Meet.* **2011**, 3361.
- ⁸R. Li, Y. Lu, S. D. Chae, G. Zhou, Q. Liu, C. Chen, M.-S. Rahman, T. Vasen, Q. Zhang, P. Fay *et al.*, *Phys. Status Solidi C* **9**, 389 (2012).
- ⁹R. Li, Y. Lu, G. Zhou, Q. Liu, S. D. Chae, T. Vasen, W.-S. Hwang, Q. Zhang, P. Fay, T. Kosel *et al.*, *IEEE Electron Device Lett.* **33**, 363 (2012).
- ¹⁰G. Zhou, Y. Lu, R. Li, Q. Zhang, Q. Liu, T. Vasen, H. Zhu, J.-M. Kuo, T. Kosel, M. Wistey *et al.*, *IEEE Electron Dev. Lett.* **33**, 782 (2012).
- ¹¹U. E. Avci, R. Rios, K. Kuhn, and I. A. Young, *Symp. VLSI Technol.* **2011**, 124.
- ¹²U. E. Avci, S. Hasan, D. E. Nikonov, R. Rios, K. Kuhn, and I. A. Young, *Symp. VLSI Technol.* **2012**, 183.
- ¹³V. V. Afanas'ev, *Internal Photoemission Spectroscopy: Principles and Applications* (Elsevier, Amsterdam, 2008).
- ¹⁴V. V. Afanas'ev and A. Stesmans, *J. Appl. Phys.* **102**, 081301 (2007).
- ¹⁵N. V. Nguyen, M. Xu, O. Kirillov, P. D. Ye, C. Wang, K. Cheung, and J. S. Suehle, *Appl. Phys. Lett.* **96**, 052107 (2010).
- ¹⁶R. Yan, Q. Zhang, W. Li, C. Irene, T. Shen, C. A. Curt, A. R. Hight-Walker, X. Liang, A. Seabaugh, D. Jena *et al.*, *Appl. Phys. Lett.* **101**, 022105 (2012).
- ¹⁷K. Nishi, N. Morota, Y. Murase, and H. Nakashima, *Nucl. Instrum. Methods Phys. Res. B* **144**, 107 (1998).
- ¹⁸R. H. Fowler, *Phys. Rev.* **38**, 45 (1931).
- ¹⁹Q. Zhang, G. Zhou, H. Xing, A. Seabaugh, K. Xu, H. Sio, O. A. Kirillov, C. A. Richter, and N. V. Nguyen, *Appl. Phys. Lett.* **100**, 102104 (2012).
- ²⁰The mention or use of products in this manuscript is not meant as an endorsement by NIST nor as an indication that they are the best available.
- ²¹R. J. Powell, *J. Appl. Phys.* **41**, 2424 (1970).
- ²²S. Tiwari and D. J. Frank, *Appl. Phys. Lett.* **60**, 630 (1992).
- ²³R. Ferrini and M. Patrini, *J. Appl. Phys.* **85**, 4517 (1998).
- ²⁴W. R. Frensley, *BANDPROF* (University Texas at Dallas, Dallas, TX, 2001).
- ²⁵O. S. Heavens, *Optical Properties of Thin Solid Films* (Academic, New York, 1955).
- ²⁶The transmittance into the InP substrate is shown with the dashed line in Fig. 5, which decreases quickly below 5% with photon energy above 3.3 eV, confirming the way we used the photon energy of (3.5–4.3 eV) to extract barrier height for InGaAs was reasonable as presented in Ref. 19.